

****Volume Title****

*ASP Conference Series, Vol. **Volume Number***

****Author****

© ****Copyright Year**** *Astronomical Society of the Pacific*

From Bipolar to Elliptical: Morphological Changes in the Temporal Evolution of PN

M. Huarte Espinosa^{1,2}, A. Frank¹, B. Balick³, O. De Marco⁴, J. H. Kastner⁵, R. Sahai⁶ and E. G. Blackman¹

¹*Department of Physics and Astronomy, University of Rochester, 600 Wilson Boulevard, Rochester, NY, 14627-0171*

²*Kavli Institute for Cosmology Cambridge, Madingley Road, Cambridge CB3 0HA, UK*

³*Department of Astronomy, University of Washington, Seattle, WA 98195*

⁴*Department of Physics, Macquarie University, Sydney NSW 2109, Australia*

⁵*Rochester Institute of Technology, 54 Lomb Memorial Drive, Rochester, NY 14623, USA*

⁶*NASA/JPL, 4800 Oak Grove Drive, Pasadena, CA 1109, USA*

Abstract. Proto-planetary nebulae (pPN) and planetary nebulae (PN) seem to be formed by interacting winds from asymptotic giant branch (AGB) stars. The observational issue that most pPN are bipolar but most older PN are elliptical is addressed. We present 2.5D hydrodynamical numerical simulations of episodic cooling interacting winds to investigate the long term evolution of PN morphologies. We track wind acceleration, decrease in mass-loss and episodic change in wind geometry from spherical (AGB) to collimated (pPN) and back to spherical again (PN). This outflow sequence is found to produce realistic PN dynamics and morphological histories. Effects from different AGB distributions and jet duty cycles are also investigated.

Keywords. Planetary Nebulae

1. Introduction

Planetary Nebulae are thick ionized plasma clouds that expand at $\sim 20 \text{ km s}^{-1}$ away from an old, hot, intermediate-mass star. The nebulae show bipolar, elliptical, point symmetric, irregular, spherical and quadrupolar morphologies (for a review see Balick & Frank 2002). The interacting stellar wind model (ISW; Kwok, Purton, & Fitzgerald 1978) suggest that spherical PN form by the collision of the dust slow dense shell around an AGB star and the tenuous fast wind that it blows at the post-AGB phase. As opposed to PN, AGB envelopes are typically spherical, therefore, PN must be shaped as they evolve, by some mechanisms which are not clear yet (Balick & Frank 2002). Generalized ISW models propose that bipolar PN form by the interaction of the post-AGB fast wind and either a toroidal AGN envelope (e.g. Frank & Mellema 1994) or an aspherical AGB wind (e.g. Icke, Balick, & Frank 1992). A binary system may cause asymmetries in the AGB wind; where either an AGB interacts with a companion or an AGB and its companion share a common envelope evolution (for a review see de

Marco 2009). Magnetic fields (e.g. Blackman, Frank, & Welch 2001), the rotation of the AGB (e.g. Garcia-Segura 1997) and photoionization heating from the central star (e.g. Mellema 1997) have also been considered in PN shaping.

Jets are evident in high resolution sensitive observations of many pPN and young PN (e.g. Balick 2000; Sahai 2000). The outflows appear to be bipolar, collimated and launched at $\sim 200 \text{ km s}^{-1}$ from the vicinities of the central star. Jets are thought to shape PN, to form knots in the nebulae and also to yield point symmetric objects (e.g. Sahai & Trauger 1998).

Here we present numerical simulations of episodic interacting winds to address the observational issue that more than 50 % of pPN are bipolar but more than 50% of older PN are elliptical.

2. Model and methodology

Numerical simulations of interacting stellar winds are presented. We track wind acceleration, mass-loss history and episodic change in wind geometry. The equations of radiative hydrodynamics are solved in two-dimensions, with axisymmetry conditions, using the adaptive mesh refinement (AMR) code AstroBEAR (Cunningham et al. 2009). We use the tables of Dalgarno & McCray (1972) to simulate optically thin cooling, ionization of H and He, and H_2 chemistry too. No gravitational or viscous or magnetic processes are considered.

The computational domain is a square representing 1 pc^2 . We use extrapolation boundary conditions in the upper, the lower and the right domain edges, and reflective conditions in the left edge. Cylindrical coordinates are used with the origin at the middle of the left boundary, $r \in (0, \sqrt{2}) \text{ pc}$ and $\theta \in (-\pi/2, \pi/2) \text{ rad}$. The grid has 128^2 coarse cells and two AMR levels; an effective resolution of $\sim 400 \text{ AU}$. We use BlueHive¹, an IBM parallel cluster of the Center for Research Computing of the University of Rochester, to run each simulation for about 20 hrs, using 16 processors.

2.1. Wind episodes

We consider three wind episodes: the isotropic AGB wind, the collimated jet and the isotropic fast (post-AGB) wind. The AGB is the initial condition. Simulation 1 follows the interaction of the AGB wind and the jet, whereas Simulation 2 follows the interaction of the AGB and the fast wind. Simulation 3 tracks the interaction of the AGB wind, the jet which is ejected afterwards and the fast wind which comes after the jet (see Table 1).

The AGB wind is set throughout the domain with an ideal gas equation of state ($\gamma = 5/3$), a temperature of 500 K, a radial velocity of 10 km s^{-1} and a mass-loss of $10^{-5} \text{ M}_{\odot} \text{ yr}^{-1}$. The jet is injected for 108 yr, only, in cells where $r < 6000 \text{ AU}$, with a collimated horizontal velocity of 200 km s^{-1} , the AGB's temperature and half of the AGB's density. The isotropic fast wind is continuously injected at $r < 6000 \text{ AU}$, with a mass-loss that decreases in time from 5×10^{-7} to $5 \times 10^{-9} \text{ M}_{\odot} \text{ yr}^{-1}$, following the model of Perinotto et al. (2004). The fast wind accelerates from 200 to 2000 km s^{-1} , maintaining a constant ram pressure, and we keep a Mach 20 condition in the injection region.

¹ https://www.rochester.edu/its/web/wiki/crc/index.php/BlueHive_Cluster

Additionally, Simulations 4, 5, and 6 follow the interaction between the jet, the fast wind or both, respectively (see Table 1), and an initial AGB with a pole-to-equator density contrast of 1/2. We use the toroidal density distribution in equations (1) and (2) of Frank & Mellema (1994)². Finally, in Simulation 7, the fast wind interacts with a spherical AGB wind having a pole-to-equator velocity contrast of 2. This is modeled by multiplying the AGB's radial velocity by $1 + e^{-[\tan^{-1}(|y/x|)/0.3]^2}$ (see Table 1).

Table 1. Simulations and parameters.

Simulation	AGB wind form	Jet duration [$\times 108$ yr]	Fast wind duration [$\times 1000$ yr]
1	spherical	1	0.0
2	spherical	0	13.0
3	spherical	1	10.7
4	toroidal ρ	1	0.0
5	toroidal ρ	0	3.8
6	toroidal ρ	1	6.0
7	aspherical \mathbf{v}	0	13.0

3. Results and discussion

We present a summary of the simulation results, for details see Huarte Espinosa et al. 2010 (in prep.). Figure 1, top row, shows the evolution of Simulation 1. The jet collides with the AGB envelope, drives a bow shock and forms a central elliptical cavity. Jet injection ceases at 108 yr and gas expands passively afterwards. The lobe develops a bipolar morphology with a monotonically increasing aspect ratio (i.e. the ratio of its longer dimension to its shorter dimension) that reaches 4.5 in 13283 yr. Conversely, Simulation 2 (middle row) follows the ISW model (Kwok, Purton, & Fitzgerald 1978) closely. The fast wind quickly overtakes the AGB envelope, drives a bow shock on it, and a hot bubble (10^{7-8} K) forms between the envelope and the working surface of the fast wind. Gas is then pushed supersonically onto the envelope, producing a compressed, spherical and efficiently-cooling shell expanding at $\sim 20 \text{ km s}^{-1}$. In Simulation 3 (bottom row), the jet forms a central bipolar cavity which is then blow form within by the isotropic fast wind. A hot bubble forms in the swept up region, bound by a compressed shell that quickly adopts an elliptical morphology and expands at $\sim 20 \text{ km s}^{-1}$ with a widely constant aspect ratio of 2. Simulation 3 shows how bipolar young PN transform into old larger elliptical nebulae, in agreement with observed PN morphological histories. In Simulations 4, 5 and 6 (not shown), the toroidal AGB envelope funnels any subsequent stellar outflow towards the pole and yields narrow-waisted bi-polar or bi-lobed objects consistently. The long term morphologies correlate with outflow histories. An elliptical rhombus-looking shell forms quickly and slowly expands homologically in Simulation 7 (not shown), where the radiative hydro evolution occurs as in Sim. 2, but for the differences in the shell shape. In complementary simulations: gas was allowed to expand passive between the jet and the fast wind episodes; Sim. 3 was allowed to expand for longer (up to 26500 yr); gas temperature was suddenly raised to 10000 K

² We use the referred equations for $\alpha = 1/2$ and $\beta = 1$.

everywhere, to crudely simulate the effects of photoionization from the central star. We found mild results in these experiments relative to the ones in Table 1.

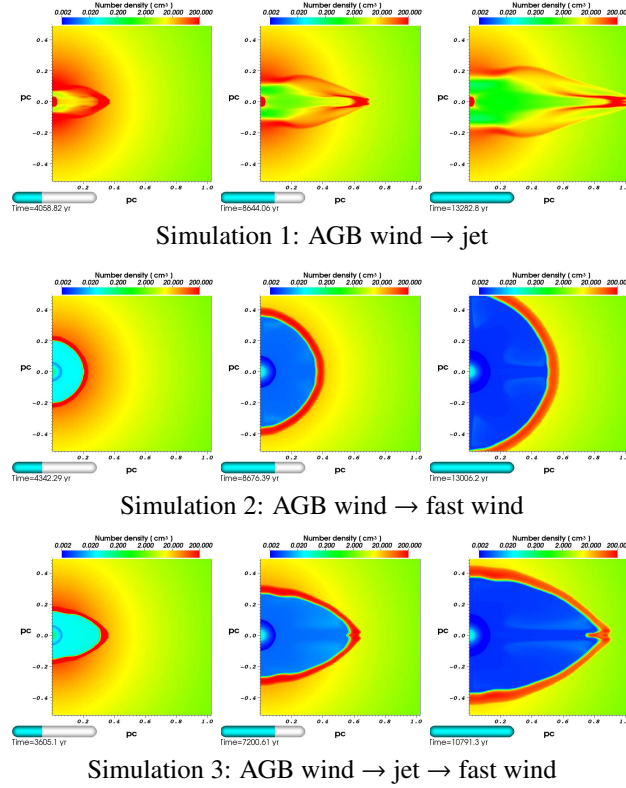


Figure 1. Evolution of the gas density in logarithmic contours. A jet produces a narrow bipolar shell. An isotropic fast wind forms a spherical shell. A jet followed by a fast wind yields an elliptical shell.

Acknowledgments. The authors wish to thank the organizers of the meeting for their work and kindness. MHE thanks Jonathan Carroll for discussions.

References

- Balick, B. 2000, in *Asymmetrical Planetary Nebulae II: From Origins to Microstructures*, edited by J. H. Kastner, N. Soker, & S. Rappaport, vol. 199 of *Astronomical Society of the Pacific Conference Series*, 41
- Balick, B., & Frank, A. 2002, *ARA&A*, 40, 439
- Blackman, E. G., Frank, A., & Welch, C. 2001, *ApJ*, 546, 288. [arXiv:astro-ph/0005288](#)
- Cunningham, A. J., Frank, A., Varnière, P., Mitran, S., & Jones, T. W. 2009, *ApJS*, 182, 519. [0710.0424](#)
- Dalgarno, A., & McCray, R. A. 1972, *ARA&A*, 10, 375
- de Marco, O. 2009, *PASP*, 121, 316. [0902.1137](#)
- Frank, A., & Mellema, G. 1994, *ApJ*, 430, 800
- García-Segura, G. 1997, *ApJ*, 489, L189+
- Icke, V., Balick, B., & Frank, A. 1992, *A&A*, 253, 224
- Kwok, S., Purton, C. R., & Fitzgerald, P. M. 1978, *ApJ*, 219, L125

- Mellema, G. 1997, A&A, 321, L29. [arXiv:astro-ph/9704172](#)
Perinotto, M., Schönberner, D., Steffen, M., & Calonaci, C. 2004, A&A, 414, 993
Sahai, R. 2000, in *Asymmetrical Planetary Nebulae II: From Origins to Microstructures*, edited by J. H. Kastner, N. Soker, & S. Rappaport, vol. 199 of *Astronomical Society of the Pacific Conference Series*, 209
Sahai, R., & Trauger, J. T. 1998, AJ, 116, 1357